SUPPLEMENTAL MATERIAL

In this Supplemental Material, we first present more details on realizing the mechanical parametric amplification (MPA) through modulating the spring constant of the cantilever with a time-dependent pump in this setup. Second, we derive the total Hamiltonian of this hybrid system and discuss the basic idea of enhancing the spin-phonon and spin-spin coupling at the single quantum level. Meanwhile, we show detailed descriptions and discussions on the validity of the effective Rabi model in this work. We also discuss one potential strategy for engineering the effective dissipation rate of the mechanical mode. Third, we discuss two specific applications of the spin-mechanical setup with the proposed method, i.e., adiabatically preparing Schrödinger cat states and entangling multiple separated NV spins via exchanging virtual phonons. Finally, we present some discussions on applying the basic idea to enhance the strain coupling between the NV spins and the diamond nanoresonator.

Realizing MPA through modulating the spring constant

In this scheme, in order to realize MPA, we apply the periodic drive to modulate the spring constant of the cantilever. This can be accomplished by positioning an electrode near the lower surface of the cantilever and applying a tunable time-varying voltage. As shown in Fig. 1(a) in the main text, the electrode materials are homogeneously coated on the lower surface of the cantilever, and another electrode plate with the tunable oscillating pump is placed just under the cantilever. The Hamiltonian of this mechanical system with the time-dependent spring constant is

$$\hat{H}_{\rm mec}=\frac{\hat{p}_z^2}{2M}+\frac{1}{2}k(t)\hat{z}^2=\frac{\hat{p}_z^2}{2M}+\frac{1}{2}k_0\hat{z}^2+\frac{1}{2}k_r(t)\hat{z}^2. \tag{S1}$$

The gradient of the electrostatic force from the electrode has the effect of modifying the spring constant according to $k(t)=k_0+k_r(t)$, with $k_0=\omega_m^2M$ the unperturbed fundamental spring constant and the time-varying pump item

$$k_r(t)\equiv\partial^2(C_rV^2)/(2\partial\hat{z}^2)=\partial F_e/\partial\hat{z}=\Delta k\cos(2\omega_pt). \tag{S2}$$

Here, $F_e=\partial(C_rV^2)/(2\partial\hat{z})$ is the tunable electrostatic force exerted on the cantilever by the electrode, $\hat{z}$ is the cantilever displacement, Δk is the variation of the spring constant, and $2\omega_p$ is the pump frequency. Therefore, these two electrode plates form a general parallel-plate capacitor, and its capacitance is $C_r=\varepsilon S/(d+\hat{z})$. Here, $\varepsilon\equiv\varepsilon_0\varepsilon_r$ is the permittivity, ε_0 and ε_r are the vacuum and the relative permittivity, respectively, S is the effective area, and $(d+\hat{z})$ is the distance between the two plates. Here we assume the voltage $V=V_0+V_p\cos 2\omega_pt$ with $V_0>V_p$. Substituting this into (S2) and keeping only the $2\omega_p$ item, we can obtain the time-varying spring constant

$$k_r(t)\simeq\frac{2V_0V_p\varepsilon S}{d^2}\times\cos 2\omega_pt. \tag{S3}$$

Defining the displacement operator $\hat{z}=z_{\rm zpf}(\hat{a}^\dagger+\hat{a})$ with the zero field fluctuation $z_{\rm zpf}=\sqrt{\hbar/2M\omega_m}$, we can quantize the Hamiltonian of the cantilever $\hat{H}_{\rm mec}$ ($\hbar=1$),

$$\hat{H}_{\rm mec}=\omega_m\hat{a}^\dagger\hat{a}-\Omega_p\cos(2\omega_pt)(\hat{a}^\dagger+\hat{a})^2, \tag{S4}$$

where $\omega_m=\sqrt{k_0/M}$ is the fundamental frequency, and $\Omega_p=-\Delta k z_{\rm zpf}^2/2$ is the nonlinear drive amplitude. As a result, utilizing this method, we obtain the second-order nonlinear drive through modulating the spring constant in time. As illustrated in Fig. S1, we plot this nonlinear amplitude Ω_p varying with the distance d between this two electrode plates.

Note that we can tune the spring constant of this mechanical resonator through modifying V, ε, S, and d. Therefore, we can assume that Δk is a time-independent constant ($\partial_t\Delta k=0$) for the case of exponentially enhancing the spin-phonon and spin-spin couplings in this spin-mechanical system. On the other hand, to ensure the adiabaticity of this dynamical process and to accomplish the adiabatic preparation of the Schrödinger cat state, we can also assume that $\Delta k(t)$ is a slowly time-varying parameter (which means $\partial_t\Delta k\approx 0$). For these two different cases, we will make specific discussions in the following sections.

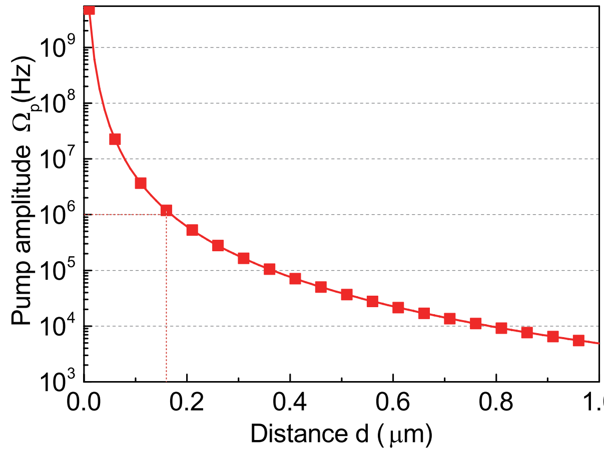

FIG. S1. (Color online) The pump amplitude Ω_p varying with the distance d between the cantilever's lower surface and the electrode plate. The parameters are set as: the static voltage $V_0 = 10\ V$, the oscillating voltage $V_p = 2\ V$, the zero field fluctuation $z_{\mathrm{zpf}} \sim 2.14 \times 10^{-13} m$, and the parallel-plate effective area $S \sim 1.0\ \mu\mathrm{m} \times 0.1\ \mu\mathrm{m}$.

The Hamiltonian for this hybrid system

The motion of the cantilever attached with the magnet tip produces the time-dependent gradient magnetic field $\vec{B}(t) = \vec{B}\cos\omega_m t$ at the corresponding NV spin, with $\vec{B} = (B_x,\ B_y,\ B_z)$ the gradient magnetic field vectors and the cantilever's fundamental frequency ω_m. Because ω_m is much smaller than the energy transition frequency ($\omega_m \ll D \pm \delta/2$), we can ignore the far-off resonant interactions between the NV spin and the gradient magnetic fields along the x and y directions. In the rotating frame at the frequency ω_m, the Hamiltonian for describing the magnetic interaction between the mechanical mode and the single NV center is

$$\hat{H}_{\mathrm{int}} = \mu_B g_e G_m \hat{z}\hat{S}_z = \lambda_0(\hat{a}^\dagger + \hat{a})\hat{S}_z, \tag{S5}$$

where $\lambda_0 = \mu_B g_e G_m z_{\mathrm{zpf}}$ is the magnetic coupling strength.

Then we apply the dichromatic microwave classical fields $B_x^{\pm}(t)$ (with frequencies ω_+ and ω_-) polarized in the x direction to drive the transitions between the states $|0\rangle$ and $|\pm 1\rangle$. The Hamiltonian for describing the single NV center driven by the dichromatic microwave fields is $\hat{H}_{\mathrm{NV}} = D\hat{S}_z^2 + \frac{1}{2}\delta\hat{S}_z + \mu_B g_e(B_x^+(t) + B_x^-(t))\hat{S}_x$, with the classical periodic driving fields $B_x^{\pm}(t) = B_0^{\pm}\cos(\omega_\pm t + \phi_\pm)$. For a single NV center, we can obtain the Hamiltonian in the rotating frame with the microwave frequencies $\omega_\pm$,

$$\hat{H}_{\mathrm{NV}} = \sum_{j=\pm} -\Delta_j |j\rangle\langle j| + \frac{\Omega_j}{2}(|0\rangle\langle j| + |j\rangle\langle 0|), \tag{S6}$$

where $\Delta_\pm \equiv |D - \omega_\pm \pm \delta/2|$ and $\Omega_\pm \equiv g_e\mu_B B_0^{\pm}/\sqrt{2}$. For simplicity, we set $\Delta_\pm = \Delta$ and $\Omega_\pm = \Omega$ in the following discussions. The Hamiltonian (S6) couples the state $|0\rangle$ to a "bright" state $|b\rangle = (|+1\rangle + |-1\rangle)/\sqrt{2}$, while the "dark" state $|d\rangle = (|+1\rangle - |-1\rangle)/\sqrt{2}$ is decoupled. The resulting eigenbasis of $\hat{H}_{\mathrm{NV}}$ is therefore given by $|d\rangle$ and the two dressed states $|g\rangle = \cos\theta|0\rangle - \sin\theta|b\rangle$ and $|e\rangle = \cos\theta|b\rangle + \sin\theta|0\rangle$, where $\tan(2\theta) = -\sqrt{2}\Omega/\Delta$. Under this dressed basis, we acquire the eigenfrequencies $\omega_d = -\Delta$, and $\omega_{e/g} = (-\Delta \pm \sqrt{\Delta^2 + 2\Omega^2})/\sqrt{2}$. The energy level diagram of the dressed spin states is illustrated in Fig. 1(c) in the main text. The parameters Ω and Δ are adjustable, and we can get the suitable energy level which is comparable with the frequency ω_m.

Therefore, we obtain the total Hamiltonian

$$\begin{aligned}\hat{H}_{\mathrm{Total}} &= \hat{H}_{\mathrm{NV}} + \hat{H}_{\mathrm{mec}} + \hat{H}_{\mathrm{int}} \\ &= \omega_m\hat{a}^\dagger\hat{a} + \omega_{eg}|e\rangle\langle e| + \omega_{dg}|d\rangle\langle d| + \frac{1}{2}(\hat{a}^\dagger + \hat{a})(\lambda|g\rangle\langle d| + \lambda^{'}|d\rangle\langle e| + h.c.) - \Omega_p\cos(2\omega_p t)(\hat{a}^\dagger + \hat{a})^2,\end{aligned} \tag{S7}$$

where the parameters are expressed as $\omega_{eg} = \omega_e - \omega_g$, $\omega_{dg} = \omega_d - \omega_g$, $\lambda = -\lambda_0\sin\theta$ and $\lambda^{'} = \lambda_0\cos\theta$. Utilizing the unitary transformation $\hat{U}_0(t) = e^{-i\hat{H}_0 t}$ with $\hat{H}_0 = \omega_p(\hat{a}^\dagger\hat{a} + |e\rangle\langle e| + |d\rangle\langle d|)$, we can simplify the Hamiltonian for this hybrid system by dropping the high frequency oscillation and the constant items,

$$\hat{H}_{\mathrm{Total}} \simeq \delta_m\hat{a}^\dagger\hat{a} + \frac{\delta_{dg}}{2}\hat{\sigma}_z - \frac{\Omega_p}{2}(\hat{a}^{\dagger 2} + \hat{a}^2) + \lambda(\hat{a}^\dagger\hat{\sigma}_- + \hat{a}\hat{\sigma}_+). \tag{S8}$$

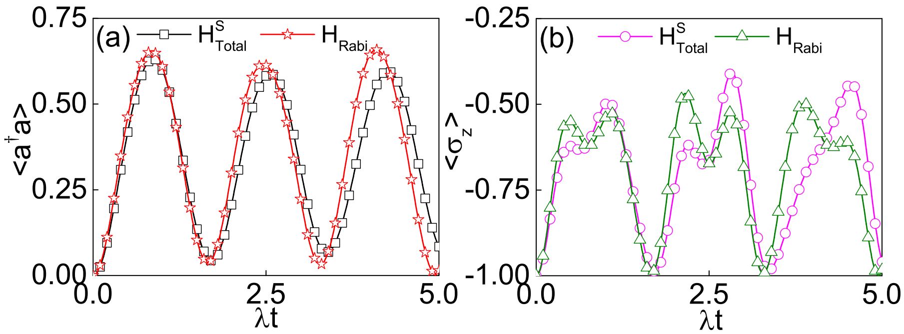

FIG. S2. (Color online) Dynamical evolution with different Hamiltonian $\hat{H}^S_{\rm Total}$ and $\hat{H}^S_{\rm Rabi}$. (a) Average phonon number $\langle \hat{a}^\dagger \hat{a}\rangle$, and (b) average spin population $\langle \hat{\sigma}_z\rangle$. Here, the initial state is $|\Psi^S(0)\rangle = |0\rangle_{\rm ph}|g\rangle$, the coefficients are $\Delta_m = 20\lambda$ and $\delta_{dg} = 2\lambda$, and the squeezing parameter is $r = 1.25$.

In this new basis $\{|d\rangle,\, |g\rangle\}$, we define $\hat{\sigma}_z \equiv (|d\rangle\langle d| - |g\rangle\langle g|)$, $\hat{\sigma}_+ \equiv |d\rangle\langle g|$, and $\hat{\sigma}_- \equiv |g\rangle\langle d|$, with $\delta_m = \omega_m - \omega_p$ and $\delta_{dg} = \omega_{dg} - \omega_p$.

Enhanced spin-phonon coupling at the single quantum level

Considering the Hamiltonian (S8), we can diagonalize the mechanical mode of $\hat{H}_{\rm Total}$ by the unitary transformation $\hat{U}_s(r) = \exp[r(\hat{a}^2 - \hat{a}^{\dagger 2})/2]$, where the squeezing parameter r is defined via the relation $\tanh 2r = \Omega_p/\delta_m$. We can obtain the Hamiltonian in the squeezed frame with the form

$$\hat{H}^S_{\rm Total} = \hat{H}^S_{\rm Rabi} + \hat{H}^S_D, \tag{S9}$$

where

$$\hat{H}^S_{\rm Rabi} = \Delta_m \hat{a}^\dagger \hat{a} + \frac{\delta_{dg}}{2}\hat{\sigma}_z + \lambda_{\rm eff}(\hat{a}^\dagger + \hat{a})\hat{\sigma}_x, \tag{S10}$$

$$\hat{H}^S_D = \frac{\lambda e^{-r}}{2}(\hat{a} - \hat{a}^\dagger)(\hat{\sigma}_+ - \hat{\sigma}_-). \tag{S11}$$

In this squeezed frame, $\hat{H}^S_{\rm Rabi}$ is the Hamiltonian for describing the Rabi model, with $\Delta_m = \delta_m/\cosh 2r$. In $\hat{H}^S_{\rm Rabi}$, we can obtain the exponentially enhanced coupling strength $\lambda_{\rm eff} \approx \lambda e^r/2$, which will be comparable with Δ_m and δ_{dg}, or even stronger than both of them when increasing r. The remaining Hamiltonian $\hat{H}^S_D$ describes the undesired correction to the ideal Rabi Hamiltonian. This item (with coefficient $\lambda e^{-r}/2$) is explicitly suppressed when we increase the squeeze parameter r, and it is negligible in the large amplification regime $1/e^r \sim 0$. Therefore, for enhancing the spin-phonon magnetic coupling through MPA, we can neglect the influence caused by $\hat{H}^S_D$ in this scheme.

To verify the discussions above, we make numerical simulations and present the results in Fig. S2. The initial state is chosen as $|\Psi^S(0)\rangle = |0\rangle_{\rm ph}|g\rangle$ for different types of Hamiltonian $\hat{H}^S_{\rm Total}$ and $\hat{H}^S_{\rm Rabi}$. Here $|0\rangle_{\rm ph}$ denotes the vacuum state of the phonon modes. The time evolution of the average phonon numbers $\hat{a}^\dagger\hat{a}$ and spin population $\hat{\sigma}_z$ is displayed in Fig. S2 (a) and (b). We find that, in spite of the negative influence caused by $\hat{H}^S_D$ in $\hat{H}^S_{\rm Total}$, the dynamical process given by $\hat{H}^S_{\rm Total}$ maintain a high degree of consistency with the standard Rabi model $\hat{H}^S_{\rm Rabi}$. Therefore, in this work, we have acquired the effective Rabi type spin-mechanical interaction with the exponentially enhanced coupling strength $\lambda_{\rm eff} \approx \lambda e^r/2$.

Here we note that, in the presence of parametric amplification, the noise coming from the mechanical bath is also amplified inevitably. This adverse factor could corrupt any nonclassical behaviour induced by the enhanced spin-motion interaction. To circumvent this detrimental effect, a possible strategy is to use the dissipative squeezing method to keep the mechanical mode in its ground state. Therefore, taking the effective dissipation rate Γ^S_m and the dephasing rate $\gamma_{\rm NV}$ into consideration, in this squeezed frame we can obtain the master equation as follow

$$\dot{\hat{\rho}} = i[\hat{\rho}, \hat{H}^S_{\rm Rabi}] + \Gamma^S_m \mathcal{D}[\hat{a}]\hat{\rho} + \gamma_{\rm NV}\mathcal{D}[\hat{\sigma}_z]\hat{\rho}, \tag{S12}$$

where $\mathcal{D}[\hat{x}]\hat{\rho} = \hat{x}\hat{\rho}\hat{x}^\dagger - \hat{x}^\dagger\hat{x}\hat{\rho}/2 - \hat{\rho}\hat{x}^\dagger\hat{x}/2$. Here we assume that the effective dissipation rate Γ^S_m is comparable with the dephasing rate $\gamma_{\rm NV}$ in the following numerical simulations.

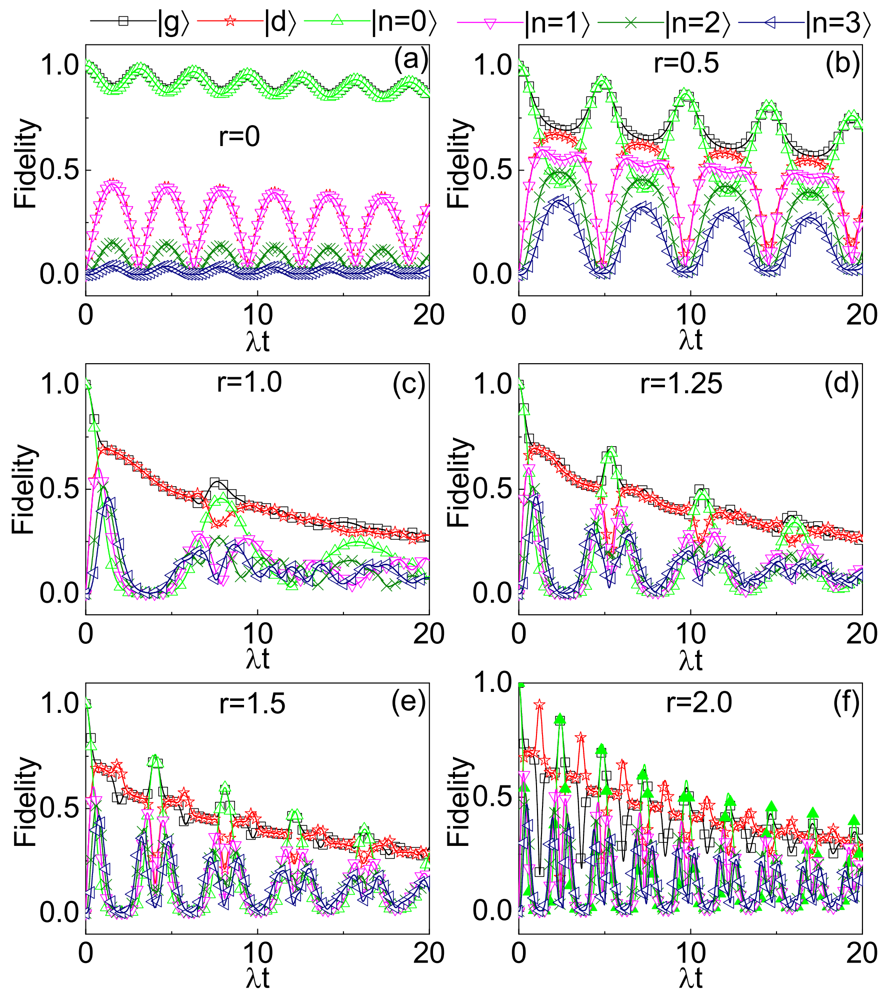

FIG. S3. (Color online) The dynamical evolution of the fidelity for different states for single NV spin ($|g\rangle$ and $|d\rangle$ correspond to the ground state and excite state) and the mechanical mode ($|n\rangle_{\rm ph}$ stands for the phonon-number state ($n = 0, 1, 2, \cdots$)), with the coefficients $\delta_m = 2\lambda$, $\delta_{dg} = 0$, and $\gamma_{\rm NV} = \Gamma_m^S = 0.01\lambda$. The different squeezed parameters correspond to (a) $r = 0$ (no squeezing), (b) $r = 0.5$, (c) $r = 1$, (d) $r = 1.25$, (e) $r = 1.5$, and (f) $r = 2.0$.

By setting the parameters as $\delta_m = 2\lambda$ and $\delta_{dg} = 0$ in Hamiltonian $\hat{H}^S_{\rm Rabi}$, we plot the time-varying fidelity for the quantum states of one NV spin ($|g\rangle$ and $|d\rangle$) and the phonon mode ($|n\rangle_{\rm ph}$, $n = 0, 1, 2, \cdots$) in Fig. S3. Here, the fidelity for the quantum states of NV spin and phonon mode are respectively expressed as $F^l_{\rm NV}(t) = \langle l|\hat{\rho}^{\rm NV}_{\rm prace}(t)|l\rangle^{1/2}$ ($l = g, d$) and $F_{\rm phonon}(t) =_{\rm ph} \langle n|\hat{\rho}^{\rm phonon}_{\rm prace}(t)|n\rangle^{1/2}_{\rm ph}$. We show that, without MAP ($r = 0$) in Fig. S3(a), we can obtain the relative weak oscillation curves for both the NV spin and the mechanical mode. However, when we increase this parameter from $r = 0.5$ to $r = 2.0$, corresponding to Fig. S3(b)-(f), the amplitude of the time-varying fidelity for the NV spin and phonon mode becomes much larger. Furthermore, the interval period for these oscillations can also be substantially shortened with the rate $\sim e^r$ when we increase r. These results indicate that, we can realize the exponentially enhanced strong spin-phonon coupling at the single quantum level in this scheme.

Engineering the effective dissipation rate in the squeezed frame

We note that in the presence of the mechanical amplification, the noise coming from the mechanical bath is also amplified. To circumvent this detrimental effect, a possible strategy is to use the dissipative squeezing approach to keep the mechanical mode in its ground state in the squeezed frame. One possible strategy is to apply an additional optical or microwave mode to this spin-mechanical system, and utilize it as an "engineered squeezed reservoir" to keep the mechanical mode in its ground state via dissipative squeezing [S1–S5]. And this steady-state technique has recently been implemented experimentally [S6–S8]. According to the basic idea from the optomechanical system, we assume this cantilever couples with an additional optical or microwave mode, and we can describe the coupled system by the Hamiltonian

$$\hat{H}_{\rm OM}=\Delta_m\hat{a}^\dagger\hat{a}+\omega_{\rm cav}\hat{c}^\dagger\hat{c}-g_0\hat{c}^\dagger\hat{c}(\hat{a}^\dagger+\hat{a})+(\alpha_+e^{-i\nu_+t}+\alpha_-e^{-i\nu_-t})\hat{c}^\dagger+{\rm H.c.} \tag{S13}$$

In which, $\hat{c}$ ($\hat{a}$) is the photon (phonon) mode annihilation operator, g_0 is the optomechanical coupling, $\nu_\pm$ and $\alpha_\pm$ are the frequency and amplitude of the two drive lasers, respectively. In the interaction picture, we apply the displacement transformation $\hat{c}=\overline{c}_+e^{-i\nu_+t}+\overline{c}_-e^{-i\nu_-t}+\hat{C}$ into Eq. (S13), with $\overline{c}_\pm$ the coherent light field amplitude due to the two lasers. Then we can linearize this optomechanical Hamiltonian as

$$\hat{H}^{\rm L}_{\rm IP}=-\hat{C}^\dagger(D_+\hat{a}^\dagger+D_-\hat{a})-\hat{C}^\dagger(D_+\hat{a}e^{-i2\Delta_mt}+D_-\hat{a}^\dagger e^{i2\Delta_mt})+{\rm H.c.} \tag{S14}$$

Here, the effective coupling $D_\pm=g_0\overline{c}_\pm$ are strengthened by the factors $\overline{c}_\pm$. Then we can assume that $D_+<D_-$ and $D_\pm>0$ without loss of generality, and apply another unitary squeezing operation $\hat{S}^{'}=\exp[\frac{r^{'}}{2}(\hat{a}^2+\hat{a}^{\dagger 2})]$ to Eq. (S14), we can get the well known optomechanical cooling Hamiltonian

$$\hat{H}^{\rm S}_{\rm IP}=-\mathcal{O}\hat{C}^\dagger\hat{a}+{\rm H.c.} \tag{S15}$$

In equation (S15) above, we have discarded the high frequency oscillation items, and the relevant definitions are $\tanh r^{'}=D_+/D_-$, $\sinh r^{'}=D_+/\mathcal{O}$, $\cosh r^{'}=D_-/\mathcal{O}$, and $\mathcal{O}=\sqrt{D_-^2-D_+^2}$. Thus, despite being driven with the classical fields, this cavity mode acts as a squeezed reservoir leading to mechanical squeezing. In this new squeezed frame, we can cool the mechanical mode into its ground state $|0\rangle_{\rm ph}$, and in its original frame, this vacuum state corresponds to the squeezed vacuum state $\hat{S}^{'}|0\rangle_{\rm ph}$.

On the other hand, in this ancillary photon-phonon interaction system, the cavity mode at here plays the role of the auxiliary engineered squeezed reservoir, which can implement an assistance on suppressing the realistic mechanical noise of this cantilever. For the realistic condition, this cavity is assumed to obey the bad-cavity limit with the large cavity damping rate κ_C, and its photon state will always stay in the vacuum state. So we can eliminate this cavity degree $\hat{C}$ and derive the Lindblad master equation for the reduced density matrix $\hat{\varrho}$ of the mechanical resonator.

$$\dot{\hat{\varrho}}=\Gamma_m^S(\hat{a}\hat{\varrho}\hat{a}^\dagger-\hat{a}^\dagger\hat{a}\hat{\varrho}/2-\hat{\varrho}\hat{a}^\dagger\hat{a}/2). \tag{S16}$$

Here, $\Gamma_m^S=4\mathcal{O}^2/\kappa_C$.

Thus, we have accomplished the target of the engineered cavity reservoir, and we can suppress the mechanical noise by utilizing the general squeezed-vacuum-reservoir technique [S9]. As a result, this additional cavity mode in this scheme acts as an engineered reservoir which can cool the mechanical resonator into a squeezed state, and we can reach the target of engineering the effective mechanical dissipation Γ_m^S.

Enhancing the phonon-mediated spin-spin interaction

We consider a row of separated NV centers (the spacing is about $\sim$ 50 nm) magnetically couple to the same mechanical mode of the cantilever, as illustrated in Fig. S4.

According to Eq. (3) in the main text, we can obtain the total Hamiltonian,

$$\hat{H}_{\rm Total}\simeq\delta_m\hat{a}^\dagger\hat{a}-\frac{\Omega_p}{2}(\hat{a}^{\dagger 2}+\hat{a}^2)+\sum_{j=1}^{N}[\frac{\delta_{dg}^j}{2}\hat{\sigma}_z^j+\frac{\lambda^j}{2}(\hat{a}^\dagger\hat{\sigma}_-^j+\hat{a}\hat{\sigma}_+^j)]. \tag{S17}$$

Applying the same unitary transformation $\hat{U}_s(r)$ to $\hat{H}_{\rm Total}$, then we can obtain the valid and effective Rabi Hamiltonian by discarding the weak interaction terms in this squeezed frame.

$$\hat{H}^N_{\rm Rabi}=\Delta_m\hat{a}^\dagger\hat{a}+\sum_{j=1}^{N}[\frac{\delta_{dg}^j}{2}\hat{\sigma}_z^j+\lambda_{\rm eff}^j(\hat{a}^\dagger+\hat{a})\hat{\sigma}_x^j]. \tag{S18}$$

For simplicity, we set $\delta_{dg}^j=0$ for each NV spin, and apply another unitary transformation $\hat{U}=\exp(-i\hat{Z})$ to $\hat{H}^N_{\rm Rabi}$ in Eq. (S18), with $\hat{Z}=i\sum_{k=1}^N\eta_k(\hat{a}^\dagger-\hat{a})\hat{\sigma}_x^k$ and $\eta_k=\lambda_{\rm eff}^k/\Delta_m$. Here we note that η_k can be considered as the Lamb-Dicke parameter used in the ion trap system. We can obtain the effective spin-spin interactions through exchanging the virtual phonons in this spin-mechanical system, with the constraint $\eta_k\ll 1$, which corresponds to $\delta_m\gg\lambda e^{3r}/4$.

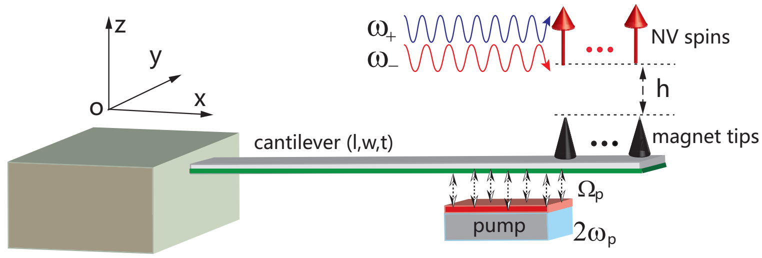

FIG. S4. (Color online) A row of magnet tips are placed at the end of the silicon cantilever.The spring constant of the cantilever is modified (pumped) at frequency $2\omega_p$ by the electric field from the capacitor plate. Moreover, the amplitude of the pump Ω_p can also be tunable. Each NV center is set just on top of the corresponding magnet tip with identical distance $h \sim 25$ nm. In addition, two microwave fields polarized in the x direction are applied to drive the NV centers between the state $|m_s = 0\rangle$ and the states $|m_s = \pm 1\rangle$.

Through using the Schrieffer-Wolff transformation $\hat{H}_{\text{eff}} = \hat{U}\hat{H}^N_{\text{Rabi}}\hat{U}^\dagger$, the mechanical mode can be eliminated from the dynamics. Then we have the following expressions

$$\hat{U}(\Delta_m \hat{a}^\dagger \hat{a})\hat{U}^\dagger = \Delta_m \hat{a}^\dagger \hat{a} - \sum_{j=1}^{N} \lambda^j_{\text{eff}}(\hat{a}^\dagger + \hat{a})\hat{\sigma}^j_x + \sum_{j,k=1}^{N} \frac{\lambda^j_{eff}\lambda^k_{eff}}{\Delta_m}\hat{\sigma}^j_x\hat{\sigma}^k_x + O(\eta^3). \tag{S19}$$

$$\hat{U}[\sum_{j=1}^{N} \lambda^j_{\text{eff}}(\hat{a}^\dagger + \hat{a})\hat{\sigma}^j_x]\hat{U}^\dagger = \sum_{j=1}^{N} \lambda^j_{\text{eff}}(\hat{a}^\dagger + \hat{a})\hat{\sigma}^j_x - 2 \times \sum_{j,k=1}^{N} \frac{\lambda^j_{eff}\lambda^k_{eff}}{\Delta_m}\hat{\sigma}^j_x\hat{\sigma}^k_x + O(\eta^3). \tag{S20}$$

Keeping only the leading order terms in η_k, we can get the effective Ising type spin-spin interactions,

$$\hat{H}_{\text{eff}} = \sum_{j,k=1}^{N} \Lambda^{jk}\hat{\sigma}^j_x\hat{\sigma}^k_x = \hat{H}^x_{\text{Ising}}, \tag{S21}$$

where $\Lambda^{jk} = \frac{\lambda^j_{\text{eff}}\lambda^k_{\text{eff}}}{\Delta_m} \approx (1 + e^{4r})\frac{\lambda^j\lambda^k}{8\delta_m}$ is the effective coupling strength between the jth NV spin and the kth NV spin. In the case of homogeneous coupling, we have

$$\hat{H}_{\text{OAT}} = \Lambda \hat{J}^2_x, \tag{S22}$$

where $\Lambda = (1 + e^{4r})\frac{\lambda^2}{8\delta_m}$, and $\hat{J}_x = \sum_{j=1}^{N}\hat{\sigma}^j_x$. This Hamiltonian corresponds to the one-axis twisting interaction or equivalently the well-known Lipkin-Meshkov-Glick (LMG) model. This one-axis twisting Hamiltonian can be used to produce spin squeezed states which generally exhibit many-body entanglement.

When we increase the squeezing parameter r, λ_{eff} will be naturally enhanced with a rate $\sim e^r$. Meanwhile, the parameter Δ_m will be reduced with a rate $\sim e^{2r}$. In order to acquire the indirect spin-spin couplings via the virtual phonon process, we require $\Delta_m \gg \lambda_{\text{eff}}$, which corresponds to the Lamb-Dicke condition $\eta_k \equiv \eta \ll 1$. To obtain the strong spin-spin coupling and ensure the validity of the virtue-phonon process, we plot the numerical results and find the valid area (the yellow area) in Fig. S5. We also point out that the yellow area with red solid dots is the optimal regime for the value of δ_m, which corresponds to the condition $0.1 \leq \eta \leq 0.2$.

Taking the effective mechanical dissipation Γ^S_m and the dephasing rate γ^j_{NV} into consideration, we can also write the master equation as follow

$$\dot{\hat{\rho}} = i[\hat{\rho}, \hat{H}^N_{\text{Rabi}}] + \Gamma^S_m\mathcal{D}[\hat{a}]\hat{\rho} + \sum_{j=1}^{N}\gamma^j_{\text{NV}}\mathcal{D}[\hat{\sigma}^j_z]\hat{\rho}. \tag{S23}$$

In the following numerical simulations, we assume that the effective mechanical dissipation rate Γ^S_m is comparable with the dephasing rate γ^j_{NV}.

Here, we take the systematic disorder into consideration for the realistic experimental implementation, and assume $\delta^j_{dq} = 0 \pm \Delta\delta^j_{dq}$ and $\lambda^j = \lambda \pm \Delta\lambda^j$ are both inhomogeneous. We constrain the disorder factors $\Delta\delta^j_{dq}$ and $\Delta\lambda^j$ to less than $\%5$ of λ. Under the Hamiltonian H^N_{Rabi} and H^x_{Ising} with different conditions (homogeneous and inhomogeneous NV spins), the simulation results for the population in the ground states $|g\rangle_j$ for these four NV centers are plotted

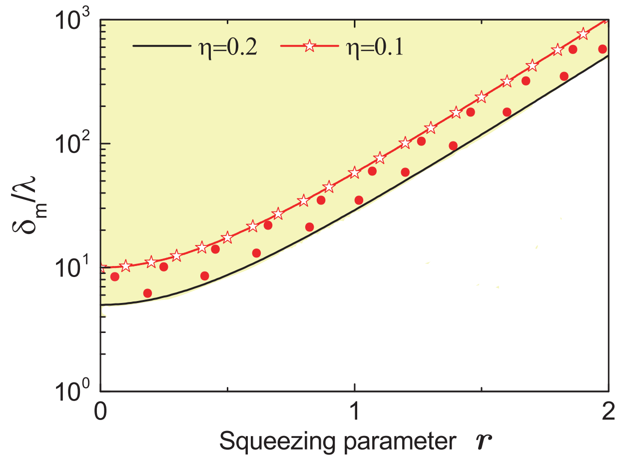

FIG. S5. (Color online) The constraint value of the parameter δ_m for achieving the effective spin-spin couplings versus the squeezing parameter r. Here, the yellow area shows the valid regime of δ_m, the black solid line and the red solid line with open star represent $\eta = 0.2$ and $\eta = 0.1$, the yellow area with red solid dots represents the regime for optimal value of δ_m varying with r.

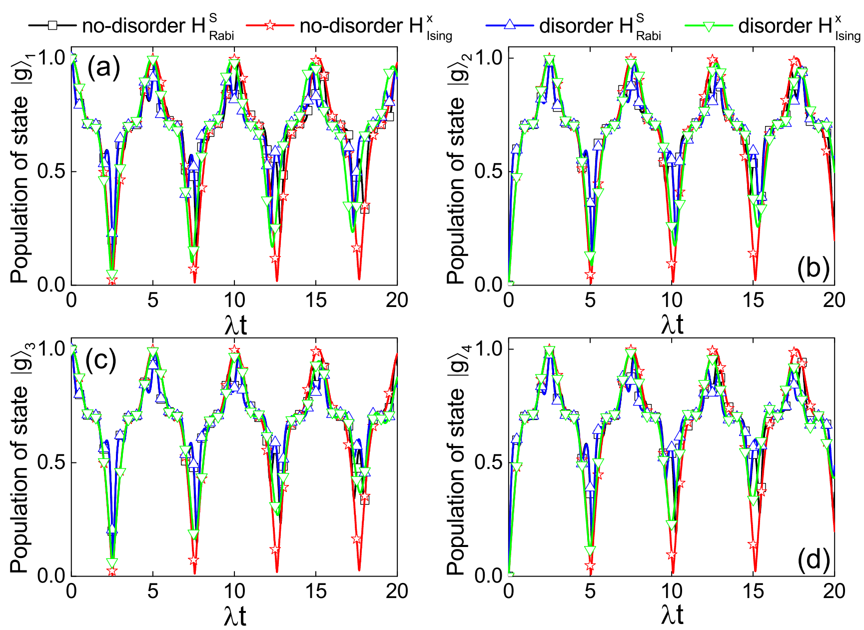

FIG. S6. (Color online) The comparison of the dynamical population for the ground states $|g\rangle_j$ of four different NV centers. (a) for state $|g\rangle_1$, (b) for state $|g\rangle_2$, (c) for state $|g\rangle_3$, and (d) for state $|g\rangle_4$, with the different Hamiltonian H^S_{Rabi} without disorder (the black solid line with open square), H^S_{Rabi} with disorder (the blue solid line with open up triangle), H^x_{Ising} without disorder (the red solid line with open star), H^x_{Ising} with disorder (the green solid line with open down triangle). Here, the initial states for this four NV spins and the phonon mode are $|g\rangle_1|e\rangle_2|g\rangle_3|e\rangle_4$ and $|0\rangle_{\mathrm{phonon}}$, respectively, and the coefficients are $r = 1.25$, $\delta_m = 60\lambda$, and $\gamma^j_{\mathrm{NV}} = \Gamma^S_m = 0.01\lambda$. For homogeneous spins (no disorder), we assume $\delta^j_{dq} = 0$ and $\lambda^j = \lambda$; while for inhomogeneous spins (disorder), we set the disorder distributions with $\{\delta^1_{dq} = -0.03\lambda,\ \delta^2_{dq} = 0.03\lambda,\ \delta^3_{dq} = 0,\ \delta^4_{dq} = -0.02\lambda\}$ and $\{\lambda^1 = 1.03\lambda,\ \lambda^2 = 0.98\lambda,\ \lambda^3 = 0.99\lambda,\ \lambda^4 = 1.01\lambda\}$.

in Fig. S6. We find that, even taking disorder into consideration, the effective Ising Hamiltonian can give rise to the results very close to those given by the Rabi Hamiltonian. Based on these results, we can accelerate the dynamical process exponentially with a rate $\sim e^{4r}$, which also provides us the most reliable and straightforward evidence for realizing the exponentially enhanced spin-spin couplings.

Preparing the Schrödinger cat state adiabatically

According to the discussions above, we can also assume that the amplitude of the pump is a slowly time-varying parameter, which can be modified slowly enough to ensure the adiabaticity during this dynamical process (the time-varying rate satisfies $\partial_t \Delta k \ll \omega_{m,p},\ \delta_m,\ \lambda$). Then Eq. (S8) can be expressed as follow

$$\hat{H}_{\text{Total}}(t) \simeq \delta_m \hat{a}^\dagger \hat{a} + \frac{\delta_{dg}}{2}\hat{\sigma}_z - \frac{\Omega_p(t)}{2}(\hat{a}^{\dagger 2} + \hat{a}^2) + \frac{\lambda}{2}(\hat{a}^\dagger \hat{\sigma}_- + \hat{a}\hat{\sigma}_+), \tag{S24}$$

where $\Omega_p(t) = -\Delta k(t) z_{\text{zpf}}^2/2$ is the time-dependent nonlinear amplitude. Here we can also diagonalize the mechanical mode in the time-dependent Hamiltonian $\hat{H}_{\text{Total}}(t)$ by the similar unitary transformation $\hat{U}_s[r(t)] = \exp[r(t)(\hat{a}^2 - \hat{a}^{\dagger 2})/2]$, with $\tanh 2r(t) = \Omega_p(t)/\delta_m$. Then we can obtain the total Hamiltonian in this time-varying squeezed frame,

$$\hat{H}^S_{\text{Total}}(t) = \hat{H}^S_{\text{Rabi}}(t) + \hat{H}^S_D(t) + \hat{H}^S_V(t), \tag{S25}$$

where

$$\hat{H}^S_{\text{Rabi}}(t) = \Delta_m(t)\hat{a}^\dagger \hat{a} + \frac{\delta_{dg}}{2}\hat{\sigma}_z + \lambda_{\text{eff}}(t)(\hat{a}^\dagger + \hat{a})(\hat{\sigma}_+ + \hat{\sigma}_-), \tag{S26}$$

$$\hat{H}^S_D(t) = \frac{\lambda e^{-r(t)}}{2}(\hat{a} - \hat{a}^\dagger)(\hat{\sigma}_+ - \hat{\sigma}_-), \tag{S27}$$

$$\hat{H}^S_V(t) = \frac{i\dot{r}(t)}{2}(\hat{a}^2 - \hat{a}^{\dagger 2}). \tag{S28}$$

Here, $\hat{H}^S_{\text{Rabi}}(t)$ is the Hamiltonian for describing the time-dependent Rabi model, with the parameter $\Delta_m(t) = \delta_m/\cosh 2r(t)$ and the coupling strength $\lambda_{\text{eff}}(t) \approx \lambda e^{r(t)}/2$. The remaining terms $\hat{H}^S_D(t)$ and $\hat{H}^S_V(t)$ describe the undesired corrections to the ideal Rabi Hamiltonian. Similar to the discussion above, the item $\hat{H}^S_D(t)$ with the coefficient $\lambda e^{-r(t)}/2$ is negligible when we increase $r(t)$. While the other correction term $\hat{H}^S_V(t)$ with the coefficient $i\dot{r}(t)/2$ vanishes explicitly with a time-independent ($\dot{r}(t) = 0$) drive amplitude. Here, we can tune the driving amplitude $\Omega_p(t)$ slowly enough to satisfy the relation $\dot{r}(t) \approx 0$. Therefore, we can also neglect the influence caused by $\hat{H}^S_D(t)$ during this dynamical process.

To confirm the discussion and analysis above, we also carry out the numerical simulations, and plot the evolution results in Fig. S7. Based on the Hamiltonians $\hat{H}^S_{\text{Total}}(t)$ and $\hat{H}^S_{\text{Rabi}}(t)$, the dynamical populations of $\hat{a}^\dagger\hat{a}$ and $\hat{\sigma}_z$ are plotted in Fig. S7(a) and (b), respectively. We find that, in spite of the negative influence caused by $\hat{H}^S_D(t)$ and $\hat{H}^S_V(t)$, the dynamical results induced by $\hat{H}^S_{\text{Total}}(t)$ are very close to those obtained from the standard Rabi model $\hat{H}^S_{\text{Rabi}}(t)$. Therefore, maintaining the adiabaticity in the whole system, $\hat{H}^S_{\text{Rabi}}(t)$ is still effective and valid to describe this spin-phonon interaction in this squeezed frame.

Considering the Hamiltonian $\hat{H}^S_{\text{Rabi}}(t)$ in Eq. (S25), we can obtain the time evolution operator as

$$\hat{\mathcal{U}}^S_{\text{Rabi}}(t) = \hat{\mathcal{T}} \exp(-i\int_0^t \hat{H}^S_{\text{Rabi}}(t^{'})dt^{'}), \tag{S29}$$

where $\hat{\mathcal{T}}$ is the time-ordering operator. By setting $\delta_{dg} = 0$ and utilizing the Magnus expansion, we can further simplify Eq. (S29) and have

$$\hat{\mathcal{U}}^S_{\text{Rabi}}(t) = e^{[\alpha(t)\hat{a}^\dagger - \alpha^*(t)\hat{a}]\hat{\sigma}_x} e^{-i\Gamma(t,0)\hat{a}^\dagger\hat{a}}, \tag{S30}$$

where the time-dependent complex parameter is expressed as $\alpha(t) = \frac{\lambda}{2i}\int_0^t e^{[r(t^{'}) - i\Gamma(t,t^{'})]}dt^{'}$, and another coefficient is $\Gamma(t,t^{'}) = \int_{t^{'}}^t \Delta_m(t^{''})dt^{''}$. We assume that this spin-mechanical system is initially prepared in the ground state $|\Psi^S(0)\rangle = |0\rangle_{\text{Phonon}}|g\rangle$, and then apply this evolution operator $\hat{\mathcal{U}}_{\text{Rabi}}(t)$ to the initial state $|\Psi^S(0)\rangle$. Finally, we can obtain the target entangled cat state of the single NV spin and the mechanical mode

$$|\Psi^S_{\text{Target}}(t)\rangle = \frac{1}{\sqrt{2}}[|\alpha(t)\rangle|+\rangle_x - |-\alpha(t)\rangle|-\rangle_x], \tag{S31}$$

where the states $|\pm\alpha(t)\rangle$ are the coherent states of the phonon mode, and the states $|\pm\rangle_x$ correspond to the two-level states in the $\hat{\sigma}_x$ representation, with the definition $|\pm\rangle_x \equiv (|d\rangle \pm |g\rangle)/\sqrt{2}$.

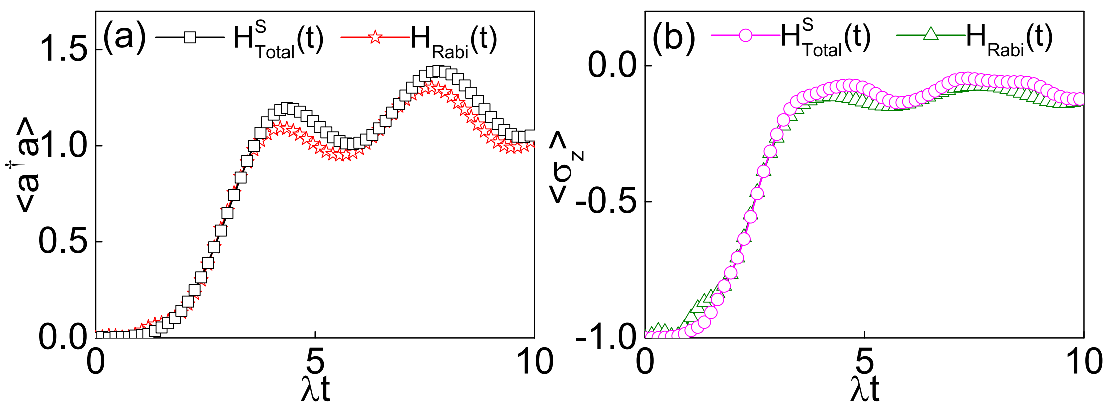

FIG. S7. (Color online) The dynamical evolution process with different types of Hamiltonian $\hat{H}^S_{\rm Total}(t)$ and $\hat{H}^S_{\rm Rabi}(t)$. (a) The population of average phonon number $\langle \hat{a}^\dagger \hat{a}\rangle$, and (b) the population of the average spin $\langle \hat{\sigma}_z\rangle$. The initial state is $|\Psi^S(0)\rangle = |0\rangle_{\rm Phonon}|g\rangle$, the coefficients are $\Delta_m(t) = \delta_m/\cosh[2r(t)]$, $\delta_m = 10\lambda$, $\delta_{dg} = 0$, $r_{\rm max} = 1.25$, and the time-dependent squeezing parameter is $r(t) = r_{\rm max}\tanh(\lambda t/2)$.

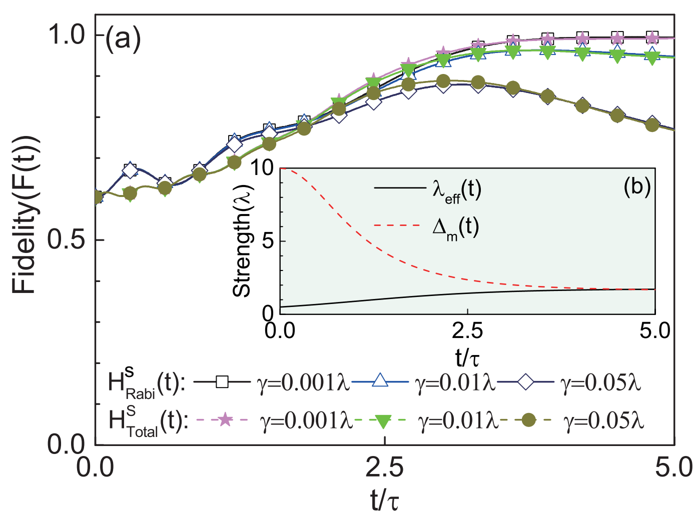

FIG. S8. (Color online) (a) The fidelity for the target entangled cat state $|\Psi^S_{\rm Target}(t_f)\rangle$ during the adiabatically dynamical evolution with different types of Hamiltonian $\hat{H}^S_{\rm Total}(t)$ and $\hat{H}^S_{\rm Rabi}(t)$ and the initial state is $|\Psi^S(0)\rangle = |0\rangle_{\rm ph}|g\rangle$. (b) The curves for the coefficient $\Delta_m(t)$ and the effective coupling $\lambda_{\rm eff}(t)$ varying with time slowly for adiabaticity. The coefficients are $\Delta_m(t) = \delta_m/\cosh[2r(t)]$, $\delta_m = 10\lambda$, $\delta_{dg} = 0$, $r_{\rm max} = 1.25$, and the time-dependent squeezing parameter is $r(t) = r_{\rm max}\tanh[t/(2\tau)]$ with $\tau = 1/\lambda$.

Therefore, during this dynamical process with the Rabi interaction $\hat{H}^S_{\rm Rabi}(t)$ from $t = 0$ to $t = t_f$, we have acquired an effective adiabatic passage between the ground state $|0\rangle_{\rm ph}|g\rangle$ and the target state $|\Psi^S_{\rm Target}(t_f)\rangle$. Here we have discarded the negligible adverse factors induced by the $\hat{H}^S_D(t)$ and $\hat{H}^S_V(t)$. To confirm this theoretical analysis and the robustness of this scheme, we make numerical simulations according to the master equation

$$\dot{\hat{\rho}} = i[\hat{\rho}, \hat{H}^S_{\rm Total/Rabi}(t)] + \gamma_{\rm NV}\mathcal{D}[\hat{\sigma}_z]\hat{\rho} + \Gamma^S_m\mathcal{D}[\hat{a}]\hat{\rho}, \tag{S32}$$

where $\gamma_{\rm NV}$ is the dephasing rate, and Γ^S_m is the effective dissipation rate in the squeezed frame. We simulate this dynamical evolution with two types of Hamiltonian $\hat{H}^S_{\rm Rabi}(t)$ and $\hat{H}^S_{\rm Total}(t)$, and plot the numerical results in Fig. S8. We find that, the fidelity reaches unity when the effective dispassion and the dephasing rate satisfy $\gamma \le 0.001\lambda$, while it decreases to 0.97 when $\gamma \le 0.01\lambda$, and then decreases to about 0.88 when $\gamma \le 0.05\lambda$. Furthermore, the dynamical fidelity obtained from $\hat{H}^S_{\rm Rabi}(t)$ (the solid line with open symbols) is in good agreement with that from $\hat{H}^S_{\rm Total}(t)$ (the solid line with solid symbols).

Entangling multiple NV spins

This spin-mechanical system with exponentially enhanced coupling strengths could allow us to carry out more complex task: entangling multiple separated NV spins through exchanging virtual phonons. Here we consider N separated NV centers (the spacing is about 50 nm ~ 0.1 μm) magnetically couple to the same mechanical mode of the cantilever. In this case, according to Eq. (S8), we can obtain the total Hamiltonian

$$\hat{H}_{\mathrm{Total}} \simeq \delta_m \hat{a}^\dagger \hat{a} - \frac{\Omega_p}{2}(\hat{a}^{\dagger 2} + \hat{a}^2) + \sum_{j=1}^{N}[\frac{\delta_{dg}^j}{2}\hat{\sigma}_z^j + \frac{\lambda^j}{2}(\hat{a}^\dagger \hat{\sigma}_-^j + \hat{a}\hat{\sigma}_+^j)]. \tag{S33}$$

Applying the same unitary transformation $\hat{U}_s(r)$ to $\hat{H}_{\mathrm{Total}}$, then we can obtain the effective Rabi Hamiltonian by discarding the weak interaction terms in the squeezed frame

$$\hat{H}_{\mathrm{eff}}^S = \Delta_m \hat{a}^\dagger \hat{a} + \sum_{j=1}^{N}[\frac{\delta_{dg}^j}{2}\hat{\sigma}_z^j + \lambda_{\mathrm{eff}}^j(\hat{a}^\dagger + \hat{a})\hat{\sigma}_x^j], \tag{S34}$$

where the coefficients are $\Delta_m = \delta_m / \cosh 2r$, $\delta_{dg}^j = \omega_{dg}^j - \omega_p$ and $\lambda_{\mathrm{eff}}^j \approx \lambda^j e^r/2$. By setting $\delta_{dg}^j = 0$ and $\lambda_{\mathrm{eff}}^j = \lambda_{\mathrm{eff}}$ for simplicity, we can obtain the Hamiltonian in the interaction picture with the form

$$\hat{H}_{\mathrm{IP}}^S = \lambda_{\mathrm{eff}}(\hat{a}^\dagger e^{i\Delta_m t} + \hat{a}e^{-i\Delta_m t})\hat{J}_x, \tag{S35}$$

in which $\hat{J}_\alpha \equiv \sum_{j=1}^N \hat{\sigma}_\alpha^j$ are the collective spin operators with $\alpha = \{x, y, z\}$.

The dynamics of the system is governed by the unitary evolution operator $\hat{U}_{\mathrm{IP}}(t) = \exp(-i\hat{H}_{\mathrm{IP}}^S t)$. Taking advantage of the Mangnus formula, we can get $\hat{U}_{\mathrm{IP}}(\tau) \simeq \exp(-i\lambda_{\mathrm{eff}}^2 \hat{J}_x^2 \tau/\Delta_m)$, with $\tau = 2\pi n/\Delta_m$ for the integer number n. This result means that the mechanical mode is decoupled from the NV spins at that moment. Note that as this operator has no contribution from the mechanical modes, thus in this instance the system gets insensitive to the states of the mechanical modes. If the system starts from the initial state $|\psi_1^S(0)\rangle = |0\rangle_{\mathrm{ph}}|gg......gg\rangle$, we can obtain the target entangled state for the N NV spins with the form $|\psi_{\mathrm{T1}}^{\mathrm{NV}}\rangle = [e^{-i\pi/4}|gg......gg\rangle + e^{i\pi/4}|dd......dd\rangle]/\sqrt{2}$, which is the well-known GHZ state.

We assume these NV centers are homogeneous and set $\delta_{dg}^j = 0$ and $\lambda_{\mathrm{eff}}^j = \lambda_{\mathrm{eff}}$ for simplicity. Then, we can obtain the Hamiltonian in the interaction picture with the form $\hat{H}_{\mathrm{IP}}^S = \lambda_{\mathrm{eff}}(\hat{a}^\dagger e^{i\Delta_m t} + \hat{a}e^{-i\Delta_m t})\hat{J}_x$. The dynamics of the system is governed by the unitary evolution operator $\hat{U}_{\mathrm{IP}}(t) = \exp(-i\hat{H}_{\mathrm{IP}}^S t)$. Taking advantage of the Mangnus formula, we can get $\hat{U}_{\mathrm{IP}}(\tau) \simeq \exp(-i\lambda_{\mathrm{eff}}^2 \hat{J}_x^2 \tau/\Delta_m)$ when $\tau = 2\pi/\Delta_m$. This means that the mechanical mode is decoupled from the NV spins at this moment. If the initial state of the NV centers is $|gg......gg\rangle$, we can obtain the target entangled state for the N NV spins with the form $|\psi^{\mathrm{NV}}\rangle = [e^{-i\pi/4}|gg......gg\rangle + e^{i\pi/4}|dd......dd\rangle]/\sqrt{2}$, which is the well-known GHZ state. The quality of the produced entangled states can be improved significantly by mechanical amplification.

Taking the effective dissipation Γ_m^S and the dephasing rate γ_{NV}^j into consideration, we have the master equation as follow:

$$\dot{\hat{\rho}} = i[\hat{\rho}, \hat{H}_{\mathrm{IP}}^S(t)] + \Gamma_m^S \mathcal{D}[\hat{a}]\hat{\rho} + \sum_{j=1}^{N}\gamma_{\mathrm{NV}}^j \mathcal{D}[\hat{\sigma}_z^j]\hat{\rho}. \tag{S36}$$

Then we can make numerical simulations on the dynamical process (to entangle the NV spins) according to equation (S36). Fig. S9 displays the fidelity F of the target entangled states and the concurrence C for the case of two NV spins varying with the evolution time and the squeezing parameter r. Starting from the initial state $|gg\rangle$, we can obtain the target entangled state of two NV spins with the form $|\psi_{\mathrm{T1}}^{\mathrm{NV}}\rangle = 1/\sqrt{2}[e^{-i\pi/4}|gg\rangle + e^{i\pi/4}|dd\rangle]$. For a fixed interaction time and in the presence of mechanical dissipation and spin dephasing, we find that, the fidelity F and concurrence C, can be improved significantly by increasing r The quality of the produced entangled state and the speed for generating it can be greatly improved.

Another application of this scheme is to engineer these collective NV spins into the spin squeezed state through the one-axis twisting spin-spin interaction. Due to the computing resources, we choose the number of the NV spins as $N \leq 10$ for numerical simulations. To quantify the spin squeezed state, we use two different spin squeezing parameters to describe this nonclassical spin state. First, we utilize the spin squeezed parameter ξ_S^2 to define the squeezing degree

$$\xi_S^2 = \frac{4\min(\Delta \hat{J}_{\vec{n}\perp}^2)}{N}, \tag{S37}$$

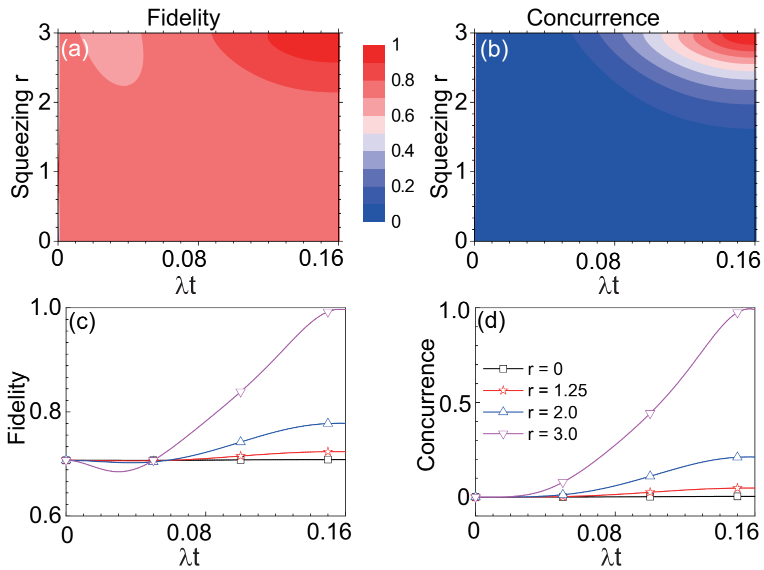

FIG. S9. (Color online) (a) and (b) Dynamical evolution of the fidelity F and the concurrence C versus the squeezing parameter r for the target entangled state, with the initial state of the NV spins $|gg\rangle$ and the coefficients $\delta_{dg}=0$, $\Delta_m=40\lambda$, and $\kappa_m^S=\gamma_{NV}=0.01\lambda$. (c) and (d) Dynamical evolution of the fidelity F and the concurrence C under different values for the squeezing parameter r.

and this definition is first introduced by Kitagawa and Ueda in 1993 [S10]. In Eq. (S37) above, $\vec{n}_\perp$ refers to an axis perpendicular to the mean-spin direction, and the term "min" is the minimization over all directions $\vec{n}_\perp$. The first step is to determine the mean-spin direction $\vec{n}_0$ by the expectation values $\langle \hat{J}_\alpha\rangle$, with $\alpha\in\{x,y,z\}$. We write $\vec{n}_0$ with spherical coordinates $\vec{n}_0=(\sin\theta\cos\phi,\sin\theta\sin\phi,\cos\theta)$, and this description is equivalent to the coherent spin state $|\theta,\phi\rangle$. We can get the other two orthogonal bases which are perpendicular to $\vec{n}_0$,

$$\begin{aligned}\vec{n}_1&=(-\sin\phi,\cos\phi,0),\\ \vec{n}_2&=(\cos\theta\cos\phi,\cos\theta\sin\phi,-\sin\theta).\end{aligned}\tag{S38}$$

Hence, $\vec{n}_\perp=\vec{n}_1\cos\beta+\vec{n}_2\sin\beta$ is the arbitrary direction vector perpendicular to $\vec{n}_0$, and we can find a pair of optimal quadrature operators by tuning β. Then we get two components of angular momentum,

$$\begin{aligned}\hat{J}_{\vec{n}_1}&=-\sin\phi\hat{J}_x+\cos\phi\hat{J}_y,\\ \hat{J}_{\vec{n}_2}&=\cos\theta\cos\phi\hat{J}_x+\cos\theta\sin\phi\hat{J}_y-\sin\theta\hat{J}_z.\end{aligned}\tag{S39}$$

As a result, we acquire the expression of optimal squeezing parameter

$$\xi_S^2=\frac{2}{N}[\langle\hat{J}_{\vec{n}_1}^2+\hat{J}_{\vec{n}_2}^2\rangle-\sqrt{(\langle\hat{J}_{\vec{n}_1}^2-\hat{J}_{\vec{n}_2}^2\rangle)^2+4\mathrm{Cov}(\hat{J}_{\vec{n}_1},\hat{J}_{\vec{n}_2})}],\tag{S40}$$

where

$$\mathrm{Cov}(\hat{J}_{\vec{n}_1},\hat{J}_{\vec{n}_2})=\frac{1}{2}\langle\hat{J}_{\vec{n}_1}\hat{J}_{\vec{n}_2}+\hat{J}_{\vec{n}_2}\hat{J}_{\vec{n}_1}\rangle.$$

On the other hand, the metrological spin squeezing parameter ξ_R^2, first introduced by Wineland et al [S11, S12], can also be applied to describe this squeezed state, with the relevant definition as

$$\xi_R^2=\frac{N(\Delta\hat{J}_\perp)^2}{\langle\hat{J}_S\rangle^2}.\tag{S41}$$

Furthermore, we note that ξ_S^2 is related to the metrological spin squeezing ξ_R^2 via $\min(\xi_R^2)=[\frac{N}{2\langle\hat{J}_S\rangle}]^2(\xi_S^2)$, with the spin length $L_{\rm spin}=\frac{|\langle\hat{J}_S\rangle|}{N/2}$. Since $|\langle\hat{J}_S\rangle|\le N/2$ and the spin length $L_{\rm spin}\le1$, so we can obtain $\xi_S^2\le\xi_R^2$. In other words, the metrological spin squeezing $\xi_R^2<1$ implies the spin squeezing $\xi_S^2<1$ according to the definition of Kitagawa and

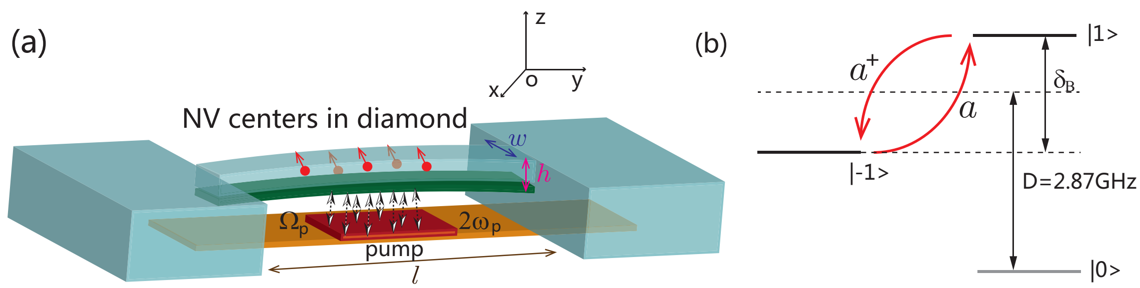

FIG. S10. (Color online) (a) The strain-induced coupling scheme with NV centers and a doubly clamped diamond nanoresonator. The spring constant of this diamond nanomechanical resonator is capacitively tunable. (b) The ground-state energy-level diagram for single NV center with the strain-mediated phonon-spin transition process($|1\rangle \leftrightarrow |-1\rangle$).

Ueda. However, the inverse is not true: we can't surely get the metrological spin squeezing $\xi_R^2 < 1$ only through the relation $\xi_S^2 < 1$ [S13–S16].

In quantum metrology, the metrological gain (the gain of phase sensitivity relative to the standard quantum limit) $G_m = (\Delta\theta_{\rm SQL}/\Delta\theta)^2$ is also a figure of merit, where the quantum standard limit $\Delta\theta_{\rm SQL} = 1/\sqrt{N}$ and the phase uncertainty $\Delta\theta = \xi_R/\sqrt{N}$ are also experimentally achieved in different systems. So we can also obtain the relation $G_m = 1/\xi_R^2$.

In a word, we can distinguish spin squeezed states or entangled spin states distinctly for multiple NV centers according to $\xi_{S,R}^2 < 1$, which also equivalently leads to the direct implications for spin ensemble-based quantum metrology applications as $G_m > 1$. And the numerical results in the main text show that these collective NV spins can be steered into the spin squeezed state more quickly as we increasing the squeezing parameter r.

Enhancing the strain-induced coupling between NV centers and nanomechanical resonators

This proposed method is also applicable for enhancing the strain-induced spin-phonon coupling through crystal strains in a diamond nanomechanical resonator. We can also achieve the spin-phonon interaction with an exponential enhancement through modifying the spring constant of the nanomechanical resonator.

As illustrated in Fig. S10(a), we consider the setup consisting of NV centers embedded in a doubly clamped diamond nanomechanical resonator, with dimensions (l, w, h). Electrodes are coated on the lower surface of the diamond nanobeam. For single NV centers, the ground-state energy level is plotted in Fig. S10(b), without classical driving, and its Hamiltonian is expressed as

$$\hat{H}_{\rm NV} = (D + d_\parallel \epsilon_\parallel)\hat{S}_z^2 + g_e\mu_B \hat{S}_z B_z - d_\perp[\epsilon_x(\hat{S}_x\hat{S}_y + \hat{S}_y\hat{S}_x) + \epsilon_y(\hat{S}_x^2 - \hat{S}_y^2)], \tag{S42}$$

where $d_\parallel$ and $d_\perp$ are the strain susceptibility parameters parallel and perpendicular to the NV symmetry axis, $\epsilon_\parallel = \epsilon_z$, $\epsilon_\perp = \sqrt{\epsilon_x^2 + \epsilon_y^2}$, and $\{\epsilon_i\}_{i=x,y,z}$ are the diagonal components of the stain tensor.

Vibration of the diamond nanoresonator periodically changes the local strain at the NV spin's position. This results in a strain-induced electric field, which will act on the corresponding NV center. Here, we focus on the resonant or near-resonant transitions between the states $|\pm 1\rangle$ caused by this strain-induced mechanical mode. Through defining $\hat{\sigma}_\pm^j = |\pm 1\rangle_j\langle \mp 1|$ and $\hat{\sigma}_z^j = |+1\rangle_j\langle +1| - |-1\rangle_j\langle -1|$ for the jth NV spin, we can get the jth NV spin's Hamiltonian in this two level subspace $\{|+1\rangle, |-1\rangle\}$ with the expression

$$\hat{H}_{\rm NV}^j = \omega_m \hat{a}^\dagger\hat{a} + \frac{\delta_B^j}{2}\hat{\sigma}_z^j + \lambda^j(\hat{a}^\dagger\hat{\sigma}_-^j + \hat{a}\hat{\sigma}_+^j), \tag{S43}$$

with ω_m the fundamental frequency of this resonator, δ_B^j the Zeeman splitting, and the coupling strength $\lambda^j/2\pi \sim 180\ \text{GHz} \times 2d_j\sqrt{\hbar/(l^3 w\sqrt{E\varrho})}/h$. For simplicity, here we assume that all of the NV centers are planted near the surface of the diamond resonator with the same distance $d_j \simeq 0.5h$.

As shown in Fig. S10(a), the electrode materials are homogeneously coated on the lower surface of the nanobeam, and another electrode with a tunable and time-varying voltage is placed just near the lower surface. The Hamiltonian of this mechanical system with the time-dependent spring constant is expressed as

$$\hat{H}_{\rm mec} = \frac{\hat{p}_z^2}{2M} + \frac{1}{2}k(t)\hat{z}^2 = \frac{\hat{p}_z^2}{2M} + \frac{1}{2}k_0\hat{z}^2 + \frac{1}{2}k_r(t)\hat{z}^2. \tag{S44}$$

The gradient of the electrostatic force from the electrode has the effect of modifying the spring constant according to $k(t) = k_0 + k_r(t)$, with $k_0 = \omega_m^2 M$ the unperturbed fundamental spring constant and the time-varying pump item $k_r(t) \equiv \partial^2(C_r V^2)/(2\partial\hat{z}^2) = \partial F_e/\partial\hat{z} = \Delta k \cos(2\omega_p t)$. Here, $F_e = \partial(C_r V^2)/(2\partial\hat{z})$ is the tunable electrostatic force exerted on the nanobeam by the electrode, $\hat{z}$ is the displacement, Δk is the drive amplitude, and $2\omega_p$ is the driving frequency. The tunable parameters $C_r = \varepsilon_0\varepsilon_r S/(d+\hat{z})$ and $V = V_0 + V_p \cos 2\omega_p t$ correspond to the electrode-nanobeam capacitance and the tunable voltage. Therefore, we can achieve

$$k_r(t) \simeq [\frac{2V_0 V_p \varepsilon S}{d^2}] \times \cos 2\omega_p t = \Delta k \times \cos 2\omega_p t. \tag{S45}$$

Defining the displacement operator $\hat{z} = z_{\mathrm{zpf}}(\hat{a}^\dagger + \hat{a})$ with the zero field fluctuation $z_{\mathrm{zpf}} = \sqrt{\hbar/2M\omega_m}$, we can quantize the Hamiltonian $\hat{H}_{\mathrm{mec}}$ ($\hbar = 1$),

$$\hat{H}_{\mathrm{mec}} = \omega_m \hat{a}^\dagger \hat{a} - \Omega_p \cos(2\omega_p t)(\hat{a}^\dagger + \hat{a})^2, \tag{S46}$$

where $\omega_m = \sqrt{k_0/M}$ is the fundamental frequency, and $\Omega_p = -\Delta k z_{\mathrm{zpf}}^2/2 = 2V_0 V_p \varepsilon S/(d+\hat{z})^2 \times z_{\mathrm{zpf}}^2/2$ is the nonlinear drive amplitude. As a result, utilizing this method, we can obtain the second-order nonlinear interaction through modulating the spring constant in time.

In this case, we can obtain the total Hamiltonian with the same expression as the magnetic coupling scheme

$$\hat{H}_{\mathrm{Total}} \simeq \delta_m \hat{a}^\dagger \hat{a} - \frac{\Omega_p}{2}(\hat{a}^{\dagger 2} + \hat{a}^2) + \sum_{j=1}^{N} [\frac{\delta_\pm^j}{2}\hat{\sigma}_z^j + \lambda(\hat{a}^\dagger \hat{\sigma}_-^j + \hat{a}\hat{\sigma}_+^j)], \tag{S47}$$

where the coefficients are respectively $\delta_m = \omega_m - \omega_p$ and $\delta_\pm^j = \delta_B^j - \omega_p$. Considering the Hamiltonian (S46), we can also diagonalize the mechanical mode by the unitary transformation $\hat{U}_s(r) = \exp[r(\hat{a}^2 - \hat{a}^{\dagger 2})/2]$. Define the squeezing parameter r via the relation $\tanh 2r = \Omega_p/\delta_m$. As a result, we obtain the Rabi Hamiltonian effectively in the squeezed frame,

$$\hat{H}_{\mathrm{Rabi}}^N = \Delta_m \hat{a}^\dagger \hat{a} + \sum_{j=1}^{N} [\frac{\delta_\pm^j}{2}\hat{\sigma}_z^j + \lambda_{\mathrm{eff}}(\hat{a}^\dagger + \hat{a})\hat{\sigma}_x^j]. \tag{S48}$$

The coefficients $\Delta_m = \delta_m/\cosh 2r$ and $\delta_\pm^j$ correspond to the free Hamiltonian of the mechanical mode and the NV spins in the squeezed frame. Furthermore, we can also obtain the exponentially enhanced spin-phonon coupling strength $\lambda_{\mathrm{eff}} \sim \lambda e^r$ in this new frame, which can be comparable with Δ_m and $\delta_\pm^j$, even stronger than both of them. As discussed in the previous section, we can easily tune the amplitude Ω_p of this nonlinear pump through modifying ε_r, $V_0 V_p$, S, and d. Therefore in this scheme we can achieve Ω_p varying with the regime from $\sim 2\pi \times 1\mathrm{kHz}$ to $\sim 2\pi \times 0.1\mathrm{GHz}$. As a result, we can explore the same idea to enhance the spin-phonon and spin-spin interactions in this strain coupling system.

[S1] Andreas Kronwald, Florian Marquardt, and Aashish A. Clerk, "Arbitrarily large steady-state bosonic squeezing via dissipation," Phys. Rev. A **88**, 063833 (2013).

[S2] P. Rabl, A. Shnirman, and P. Zoller, "Generation of squeezed states of nanomechanical resonators by reservoir engineering," Phys. Rev. B **70**, 205304 (2004).

[S3] Nicolas Didier, Farzad Qassemi, and Alexandre Blais, "Perfect squeezing by damping modulation in circuit quantum electrodynamics," Phys. Rev. A **89**, 013820 (2014).

[S4] Huatang Tan, Gaoxiang Li, and P. Meystre, "Dissipation-driven two-mode mechanical squeezed states in optomechanical systems," Phys. Rev. A **87**, 033829 (2013).

[S5] J. I. Cirac, A. S. Parkins, R. Blatt, and P. Zoller, ""Dark" squeezed states of the motion of a trapped ion," Phys. Rev. Lett. **70**, 556 (1993).

[S6] E. E. Wollman, C. U. Lei, A. J. Weinstein, J. Suh, A. Kronwald, F. Marquardt, A. A. Clerk, and K. C. Schwab, "Quantum squeezing of motion in a mechanical resonator," Science **349**, 952 (2015).

[S7] J.-M. Pirkkalainen, E. Damskägg, M. Brandt, F. Massel, and M. A. Sillanpää, "Squeezing of quantum noise of motion in a micromechanical resonator," Phys. Rev. Lett. **115**, 243601 (2015).

[S8] F. Lecocq, J. B. Clark, R. W. Simmonds, J. Aumentado, and J. D. Teufel, "Quantum nondemolition measurement of a nonclassical state of a massive object," Phys. Rev. X **5**, 041037 (2015).

[S9] Xin-You Lü, Ying Wu, J. R. Johansson, Hui Jing, Jing Zhang, and Franco Nori, "Squeezed optomechanics with phase-matched amplification and dissipation," Phys. Rev. Lett. **114**, 093602 (2015).

[S10] Masahiro Kitagawa and Masahito Ueda, “Squeezed spin states,” Phys. Rev. A **47**, 5138–5143 (1993).
[S11] D. J. Wineland, J. J. Bollinger, W. M. Itano, F. L. Moore, and D. J. Heinzen, “Spin squeezing and reduced quantum noise in spectroscopy,” Phys. Rev. A **46**, R6797–R6800 (1992).
[S12] D. J. Wineland, J. J. Bollinger, W. M. Itano, and D. J. Heinzen, “Squeezed atomic states and projection noise in spectroscopy,” Phys. Rev. A **50**, 67–88 (1994).
[S13] Peter Groszkowski, Hoi-Kwan Lau, C. Leroux, L. C. G. Govia, and A. A. Clerk, “Heisenberg-limited spin-squeezing via bosonic parametric driving,” (2020), arXiv:2003.03345 [quant-ph].
[S14] Luca Pezzè, Augusto Smerzi, Markus K. Oberthaler, Roman Schmied, and Philipp Treutlein, “Quantum metrology with nonclassical states of atomic ensembles,” Rev. Mod. Phys. **90**, 035005 (2018).
[S15] Kevin C. Cox, Graham P. Greve, Joshua M. Weiner, and James K. Thompson, “Deterministic squeezed states with collective measurements and feedback,” Phys. Rev. Lett. **116**, 093602 (2016).
[S16] W. Wang, Y. Wu, Y. Ma, W. Cai, L. Hu, X. Mu, Y. Xu, Zi-Jie Chen, H. Wang, Y. P. Song, H. Yuan, C.-L. Zou, L.-M. Duan, and L. Sun, “Heisenberg-limited single-mode quantum metrology in a superconducting circuit,” Nat. Commu. **10**, 4382 (2019).